Faculty of Engineering MEng in Engineering Design

Agrivoltaics: A Yield Prediction Model for Design Optimisation

Capstone Design Project: Individual Annex

Frank Panton

1922384

Thursday 2nd May, 2024

Acknowledgements

I would like to thank Mervyn White for his continued support throughout this project and for providing a seemingly never-ending list of ideas over the many hours we have spent discussing it. A special thanks also goes out to the other members of this project, Aasav Patel, Ellie Carey, Esi Balaban and Jack Cooper, whose enthusiasm and hard work did not waver making them a pleasure to work with.

DECLARATION

The accompanying research project report entitled: Agrivoltaics: A Yield Prediction Model for Design Optimisation is submitted in the fifth year of study towards an application for the degree of "Master of Engineering" in Engineering Design at the University of Bristol. The report is based upon independent work by the candidate. All contributions from others have been acknowledged above. The views expressed within the report are those of the author and not of the University of Bristol.

I hereby declare that the above statements are true.

Signed (author)

Full Name

FRANK PANTON

Date

02/05/2024

Contents

List of Figures

List of Tables

1 Introduction

1.1 The trade-off between agricultural yield and electrical yield

At the core of this investigation is a pivotal question: How can the balance between agricultural and electrical yields be effectively managed within agrivoltaic systems? Both yields depend critically on the same source, solar energy, requiring a precise arrangement of the system's architecture to maximise the benefits of both. A dense configuration of panels might produce substantial electrical energy but could also cast excessive shade, potentially inhibiting crop growth. Conversely, a layout with greater spacing may facilitate healthier crop development but at the cost of reduced electrical output. The inherent trade-off between agricultural and electrical yields within agrivoltaic systems has site-specific influences, such as the geographical location, which affects the angle at which solar irradiance is received, and the crops' sensitivity to sunlight. These influences necessitate the thoughtful implementation of the versatile agrivoltaic design outlined in Annex A, for a specific site, to ensure the system meets one of the project's overarching mission objectives, to 'optimise dual land use to increase land efficiency, maximising agricultural and electrical yield.'

1.2 The modelling solution

A previous branch of this research project provided a baseline for how mathematical modelling could be used to predict electrical and agricultural yields of an agrivoltaic scenario based on varying positions of solar panels [1]. The results supported the feasibility of developing a comprehensive agrivoltaic simulation tool that can explore a wide range of configurations of the modular agrivoltaic design developed in Annex A, and for a specific site, simulate the impact on both electrical and agricultural generation.

Successful modelling would not only investigate solar generation and crop generation, which both have established modelling frameworks, but fundamentally capture the effects of co-locating these systems on the same land. This requires incorporating the impact of an agrivoltaic structure on the microclimate beneath and how this influences the environmental conditions necessary for crop growth, with this modelling research conducted in Annex C. In addition, the modelling must incorporate the impact of the solar tracking algorithm developed for agrivoltaic scenarios as outlined in Annex B, which directly influences the solar power generation and the shade received by the crops. The combined modelling must provide a nuanced analysis of how changes in system design influence all aspects of modelling to provide justified and thorough insights into the optimal agrivoltaic layout.

In essence, agrivoltaic modelling serves as a powerful tool for decision-making, enabling the design of systems that achieve an optimal balance between electrical output and agricultural productivity. By simulating various scenarios and configurations, the most efficient and sustainable approaches for each specific site can be identified, maximising overall performance and benefits, and providing justified predictions to inform financial modelling.

1.3 Project aims

The primary objective of this project is to develop a bespoke model tailored to the specific design outlined in Annex A, integrating various aspects of modelling from within the overarching study. This model aims to reveal the relationships between different system design parameters, such as module height, row spacing between modules, and the number of panels per module. These insights are crucial for supporting the decision-making process to determine the optimal configuration of the developed agrivoltaic design for particular sites. Additionally, the model will provide associated yield data that informs future productivity assessments and financial projections.

2 Modelling Development

2.1 Combined Modelling Approach Methodology

A comprehensive modelling tool has been developed that integrates all aspects of modelling from this report, alongside Annex B and Annex C, with the complete algorithm flow diagram displayed in Appendix A.1.2. For a specific site, the system layout is defined by variables such as the number of panels per module, module height, row spacing, the selected tracking algorithm, and the deployment of crop protection mechanisms. This is combined with a range of environmental inputs such as weather data and farmer-specified inputs like crop types and harvest dates, resulting in a fully defined set of input variables as outlined in A.1.1.

The model begins by calculating the photovoltaic (PV) output electrical power, utilising the power and solar tracking calculations from Annex B. Simultaneously, the resultant crop yield is calculated, assisted by the microclimate modelling detailed in Annex C. The computed electrical and agricultural yields are stored alongside the associated array parameters. These parameters are then systematically adjusted, and the model is re-run to provide a thorough investigation into how yields vary as a function of array parameters. This methodical approach enables the model to offer valuable insights into optimising the agrivoltaic system configuration to maximise both electrical output and agricultural productivity.

To ensure seamless integration of all models described in Annex B and Annex C, this study employs MATLAB for comprehensive model development. MATLAB's strong numerical computation capabilities are ideal for the intricate geometrical shading calculations required by this model. Its extensive library of toolboxes provides essential tools for numerical analysis, data manipulation, and optimisation, which streamline the development process. Furthermore, the model automatically extracts most of the input variables directly through application programming interfaces (APIs), eliminating the need for manual data processing and significantly accelerating the modelling process. This integration leverages MATLAB's capabilities as a complete development environment, perfectly aligning with the requirements of this comprehensive agrivoltaic modelling project.

2.2 Electrical Yield Integration

For a given set of agrivoltaic system parameters, the type of tracking algorithm is defined, such as standard solar tracking or agriculturally sensitive algorithms tailored to co-optimise crop and energy production (further details in Annex B). The simulation tool then calculates the PV power for a single panel over the analysed time period, using the methodology outlined in Annex B. This panel power value is then scaled for the entire array, considering the defined number of panels per module and row spacing, thereby enabling the determination of the full agrivoltaic installation's output power for the size of the field. This process is carried out across a wide range of field layouts, with the results stored for further analysis. Once the optimal field layout has been identified, additional calculations for cabling losses are applied to this specific architecture as detailed in Annex B, refining the overall efficiency and effectiveness of the electrical output model.

2.3 Crop Modelling and Microclimate Modelling Integration

The integration of agrivoltaic systems affects agricultural yield in two key ways. Initially, the shading from the panels reduces the amount of solar radiation that reaches the crops. Additionally, it creates a modified micro-climate under the structure that can be fine-tuned to enhance conditions favourable for plant growth. Given that factors like sunlight, water, and temperature are vital for crop growth, accurately modelling their interplay within this altered environment is crucial for predicting agricultural yields effectively.

2.3.1 Shading of the Agrivoltaic Structure Calculation

To model the shading effects of the agrivoltaic structure on crops, the geometry of the structure was constructed in MATLAB. The agrivoltaic module, as detailed in Annex 1, was imported into MATLAB as individual components and assembled to form the full array as shown in Figure 1, allowing for adjustments in the number of panels per module, row separation, and panel rotation according to the tracking algorithm described in Annex B, which rotates the top section of the geometry to the desired rotation angle at that time step. The ground beneath was divided into a mesh of nodes within the defined study area, with the resolution of this mesh affecting its density. This setup facilitates the calculation of shading on the ground by the agrivoltaic array at each time step, accurately determining the reduced irradiance received by the crops at each node.

After defining the structure's geometry, the impact of the agrivoltaic structure on reducing irradiance levels received by the crops through shading was computed. The total irradiance received by the crops combines the direct/beam component and the diffuse component of radiation, as investigated in previous studies within this project [1]. A custom-developed ray tracing algorithm was utilised for direct shading calculations and a shading scenario was visualised in Figure 1b. The details of these geometrical calculations are further outlined in Appendix B.1. For the diffuse component, the reduction factor of diffuse irradiance is calculated, which represents the ratio of the structure's surface area to the total area of the surrounding region (detailed in Appendix B.2). This factor remains constant for a fixed panel set-up throughout the year.

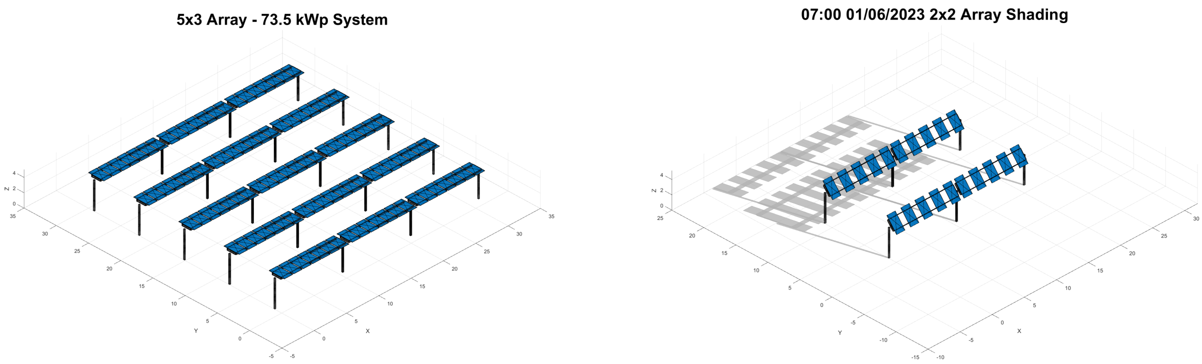

Figure 1: a) Visualisation of a 5x3 array of modules developed in MATLAB, b) The direct shading of a 2x2 array at 07:00 on the 01 of June showing the panels tilted towards the sun due to the tracking algorithm.

The results from these calculations provide the levels of irradiance received by the crops and the microclimate below, which are then used as essential inputs for modelling both the agricultural yield and the microclimate adjustments within the agrivoltaic system. The key assumptions of this modelling investigation have been detailed in Table 1, with a more complete list of assumptions and approximations outlined in Appendix D.1 with the associated potential impacts.

Table 1: Key Assumptions in Shading Modelling

No.	Assumption	Reason/Justification
1	Diffuse Irradiance is Isotropic	Assumes uniform distribution of diffuse light in all directions, common in radiation models [2]. Treating diffuse irradiance as isotropic simplifies modelling calculations.
4	Static Sun Position	The model increments the sun's position and irradiance based on available data of hourly solar position and irradiance. This does not account for the continuous movement of the sun, causing small rounding errors, however, significantly reduces computation time.
5	Simplification of Geometry	The complete agrivoltaic module geometry has been simplified for modelling purposes, overlooking real-world components such as motors and electrical cabling, slightly underestimating the shading impact of the structure.

2.3.2 Microclimate Modelling integration

The reduced irradiance data from shading calculations is a key input to the microclimate modelling detailed in Annex C. This modelling generates outputs such as temperature variations and evapotranspiration rates beneath the agrivoltaic structure. These outputs are vital for accurately modelling agricultural yield and fine-tuning microclimate settings to optimise crop growth. This data facilitates a comprehensive assessment of the environmental and biological responses to the implementation of various agrivoltaic structures.

2.3.3 Crop Growth Model

The final aspect of the modelling utilises the SIMPLE model to calculate crop yield by evaluating how effectively crops convert intercepted radiation into biomass [3]. This intercepted radiation is provided by the photosynthetically active portion [4] of the solar irradiance calculated in Section 2.3.1. Chosen for its simplicity in application and adaptability across 14 different annual crops, this model calculates yield based on daily biomass accumulation throughout the harvest period, influenced by radiation, temperature, water stress, heat stress, and atmospheric CO_2 levels, with details provided in Appendix C.

A key agrivoltaic influence in this model is the regulation of temperature and reduction of evapotranspiration due to the agrivoltaic structure, as outlined in Annex C. These factors help mitigate heat and water stress, enhancing daily growth and ultimately increasing yield. This approach ensures that the crop modelling thoroughly assesses the environmental impacts on growth, incorporating both the shading effects on radiation interception and the climatic benefits provided by the agrivoltaic system. The key assumptions of this modelling investigation have been detailed in Table 2, with a complete list of assumptions and approximations outlined in Appendix D.2.

Table 2: Key Assumptions in Crop Modelling

No.	Assumption	Reasoning/Justification
1	Constant CO2 Levels	Assumes that the available CO2 concentration remains stable throughout the modelling period at atmospheric levels [5], simplifying the CO2 availability function, and potentially overlooking small reductions in CO2 availability in the microclimate due to lack of airflow, which would reduce growth.
2	Homogeneous Crop Canopy	Assumes a homogeneous crop canopy across the field. Simplifies analysis but may not accurately represent real-world conditions where variations in plant height, health, and density exist, causing differences in light interception.
3	Lack of Crop Nutrient Dynamics	The model does not account for crop nutrient dynamics due to the significant complexity and local input data required. This may lead to an underestimation of yield or growth potential in nutrient-deficient soils such as in developing countries where soil nutrient inputs are less common.

3 Validation

This section outlines the validation process for the bespoke agrivoltaic modelling tool developed in this research. Due to its comprehensive nature, encompassing tracking algorithms, structure shading effects, and microclimate modelling for yield estimations, there are no available industry examples of this type of agrivoltaic modelling. Consequently, each component of the model undergoes individual validation to ensure accuracy and reliability. This validation provides confidence in the subsequent results and conclusions drawn, justifying its influence on the site-specific implementation layout of the modular agrivoltaic design. The validation of the electrical power generated by the solar panels is discussed in Annex B where this aspect of modelling was developed. In this model, this value is scaled to the number of solar panels within the layout and then system losses are applied as explained in Annex B, therefore this validation is not repeated in this report.

3.1 Shading Modelling Validation

The validation of the shading modelling in this study is paramount, as the solar radiance received under the structure serves as an input to both the microclimate and crop growth modelling. A shading factor was employed to quantify the reduction in irradiance caused by the agrivoltaic structure, representing the ratio of the amount of solar radiation blocked by the structure to the total solar radiation. Therefore, a shading factor of 100% represents all of the incoming light being blocked by the structure. The modelling of shading was conducted using data from a case study in Spain, allowing for a comparison of the calculated shading factor with reported values from existing literature.

Additionally, a sensitivity analysis was carried out to confirm the intuitive trend that increasing the density of the array leads to a greater reduction in solar irradiance received by the ground below. This analysis involved maintaining a constant number of panels per module while varying the row spacing from 5m to 20m separation. 5m is set as the lower limit because this is the minimum distance calculated before inter-row shading would cause significant reductions in PV power generation. Adjusting how closely packed the modules are in this way alters the ground coverage ratio (GCR), which represents the proportion of ground area covered by the array. A GCR of 1.0 indicates complete coverage of the area in agrivoltaic modules.

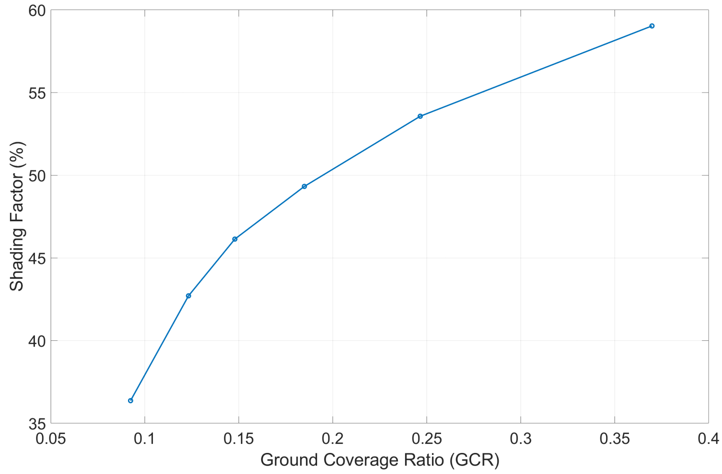

Figure 2: The Relationship between Ground Coverage Ratio (GCR) and Shading Factor.

The results of this analysis, illustrated in Figure 2, indicate a positive correlation between the ground coverage ratio and the shading factor. As GCR increases, the shading factor also increases, suggesting that as more ground is covered by solar panels (or the agrivoltaic module), the shading over the crops beneath increases which is intuitive. Figure 2 also demonstrates that as GCR increases and the layout of modules becomes more dense the rate at which shading increases, slows down. This is because the irradiance received by the ground as a result of diffuse light entering the sides of the array becomes a larger portion of the total light received by a certain point on the ground. For this study, the area was only 50m x 50m. Therefore the amount of light entering the sides of the array under the 4m module height, is significant compared to the total surface area of the array, and this diffuse light let through the sides of the array does not change as GCR increases. Whereas for large installations with wide areas, the shading percentage would tend closer towards 100% for high GCR values, because the light entering the sides is insignificant compared to the total area of the array.

The shading values depicted in Figure 2 were compared to reductions in solar irradiance reported in agrivoltaic studies, providing a form of validation by ensuring a reasonable level of similarity between modelled and literature data. Agrivoltaic research has suggested average reductions in solar radiation of around 30% [6], which aligns reasonably well with the findings of this modelling. The higher shading results in Figure 2, between 36% and 59%, are likely due to the design of the agrivoltaic module, which incorporates a solar tracking system ensuring a consistent perpendicular angle to solar irradiance. This maximises the level of shading compared to typical fixed tilt agrivoltaic structures detailed in [6]. The similarity between reported and modelled data, alongside the validation of the trend of increasing shading for denser agrivoltaic layouts, justifies the application of this modelling section to subsequent investigations in this report.

3.2 Crop Modelling Validation

The crop modelling validation focuses on two distinct geographical and crop scenarios; tomatoes in Spain and wheat in the southern UK, to demonstrate the adaptability and effectiveness of the modelling approach. The models require a significant range of crop-specific input parameters, referencing sources for tomato [7] and wheat growth data [8], alongside irradiance data from PVGIS [9] and additional weather parameters from [10].

The validation process began by comparing empirical data for expected crop yields to a modelled open-field scenario without agrivoltaic structures or irrigation. The expected yields were 80.88 t/ha [11] for Spanish tomatoes and 8.59 t/ha [12] for UK wheat. However, the model outputs showed that both crops were underestimated by 19% for tomatoes and 11% for wheat. Given the complex nature of dynamic crop modelling, these deviations are within acceptable margins. This underestimation is likely because the models do not make specific irrigation assumptions, leading to some degree of drought stress after periods without rain, informed by the precipitation data input file. Furthermore, this deviation could be attributed to variations in cultivars between those available in the model, tending to be 'average' crop cultivars, compared to the specific type grown locally.

The subsequent simulation introduced an agrivoltaic system to both scenarios, with 6m row spacing and four panels per module at a height of 4m. This resulted in a yield decrease of 28% for tomatoes and 33% for wheat compared to the open field simulation. The primary cause of this reduction is the decreased light availability, crucial for crop growth. However, tomatoes showed slightly better resilience to shading than wheat. This resilience in tomatoes could be attributed to the microclimate under the agrivoltaic structures which is captured within this model through the algorithm developed in Annex C, which likely moderated maximum temperatures and reduced heat stress. Additionally, the shading provided by the panels lowered the water loss through transpiration for both plants, reducing drought stress, which is a more significant stress factor for tomatoes compared to wheat. These factors are captured in the crop model, helping explain the differential impact on the two crops under the same agrivoltaic structure.

To further test the robustness of the crop models, the simulations were adjusted to incorporate constant irrigation, eliminating the variable of drought stress. This modification led to a dramatic increase in productivity, with a 57% yield increase for tomatoes in Spain and a 24% increase for wheat in the UK, underscoring the critical role of irrigation in mitigating drought stress and boosting crop growth, especially in water-limited environments like Spain. The pronounced increase in yield for Spanish crops highlights their frequent exposure to water stress, validating the model's ability to accurately simulate various scenarios based on irrigation availability. In contrast, the wetter climate of the UK results in wheat that is less dependent on additional irrigation, as evidenced by the smaller yield increase. This discrepancy confirms the model's effectiveness in linking microclimate modelling with drought stress impacts, demonstrating its accuracy and versatility in predicting agricultural productivity under varied environmental conditions, proving its value in effective agricultural planning.

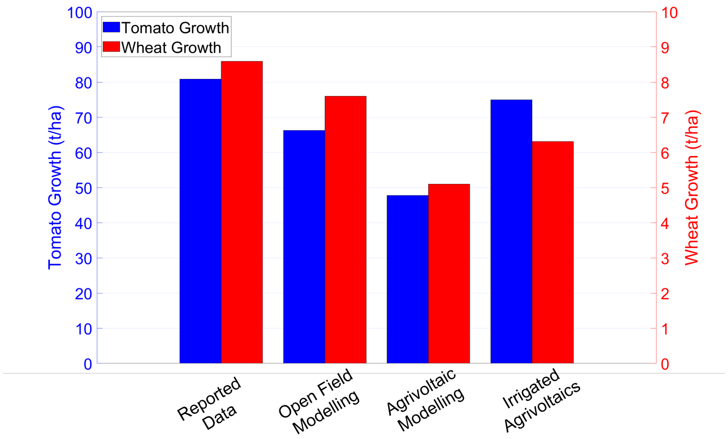

Figure 3: Tomato yield in Spain and wheat yield in the UK from, reported data for yield, modelled yield for an open field, modelled yield including an agrivoltaic structure, modelled yield for fully irrigated scenario.

The validation of the crop model confirms its effectiveness in simulating diverse agricultural scenarios, from varying irrigation practices to the integration of agrivoltaic systems. Its ability to accurately evaluate how design parameters such as module height, row spacing, and panel count impact crop growth showcase its utility. Although the trends presented in the modelling represent those of literature, there is an identified level of absolute error between modelled and reported data, therefore future modelling studies will be assessed as a percentage change from the maximum expected yield, which provides a simple comparison between the impacts of different agrivoltaic architecture variables on crop growth for design decisions, and allows for calibration to expected crop growth for application of the yields to financial modelling. In summary, this model is proven to capture variations in crop yield as a result of design decisions justifying its application to the subsequent results stages of this report.

4 Results

The results section of this report leverages the fully validated agrivoltaic modelling tool to assess the influence of varying design parameters and provides critical insights into the optimal design and implementation of the agrivoltaic modules. By simulating these scenarios, the model demonstrates its practical application and utility in informing design decisions and enhancing financial projections.

4.1 Analysis of Module Height as a Variable

The results section begins by examining the variable of height within agrivoltaic systems. Module height can be adjusted to accommodate various farming practices and optimise the balance between photovoltaic and agricultural yields. To provide specific insights into how height adjustments impact site-specific outcomes and how best to design for these, this study has explored its effects in conjunction with changes in row spacing. The analysis presented in Figure 4 highlights the dual impacts of modifying module height and row spacing on electrical yield, measured in kWh per year, and agricultural productivity of tomatoes as a percentage of the maximum modelled yield under open field conditions. This study was carried out for an agrivoltaic structure equipped with 4 panels per module, for a case study located in Spain.

From Figure 4a, it is observed that electrical yield is inversely correlated with row spacing; maximum electrical yield is achieved with minimal row spacing, and it diminishes as row spacing increases because fewer rows can fit into the 100m field, thus lowering electrical generation. Additionally, it is noted that for a given row spacing, variations in the height of the structure do not impact this output, as factors such as the number of panels and their orientation, which directly affect electrical output, remain unchanged by structure height.

Figure 4b illustrates that agricultural yield positively correlates with row spacing, starting at a lower value for small spacings and increasing as panel separation enlarges. This enhancement in yield is due to increased sunlight reaching the crops, a relationship that is consistent with previous findings regarding shading and coverage levels shown in Figure 2. Interestingly, agricultural yield also improves as the height of the structure increases for a specific row spacing. However, this effect is less pronounced than that of row spacing with an average of a 9% increase in agricultural yield from 2m to 5m height for a given row spacing, suggesting that height is a less influential variable on growth. The increase in height allows more diffuse light to penetrate the sides of the array, contributing to this observed effect in crop yield.

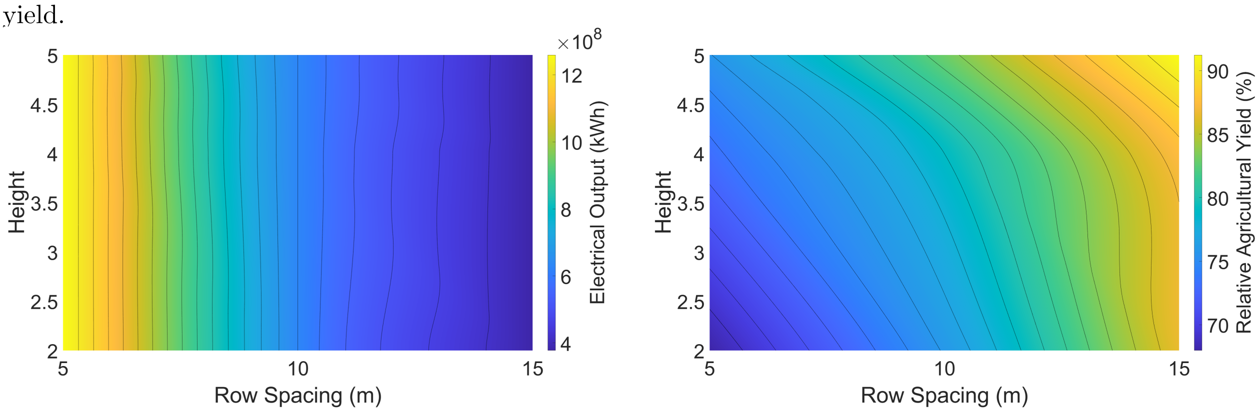

(a) Yearly electrical energy as a function of structure height (m) and row spacing (m).

(b) Relative agricultural yield as a function of structure height (m) and row spacing (m).

Figure 4: Comparison of the effects of changing structure height and row spacing on both electrical and agricultural yield.

4.1.1 Height Variation Discussion

The data presented in Figure 4 suggests that the height of the module is a less significant variable than row spacing due to not providing benefit to electrical yield and its minimal impact on agricultural yields. Therefore, as a design variable, height should be dictated by the constraints of the farming practices rather than used to generate extra yield. The height should meet requirements such as the necessary clearance for farming machinery, and comply with standards like the German requirement for a minimum of 2 meters clearance for electrical wiring in agrivoltaic systems [13]. However, it should not be increased beyond site-specific requirements, as the increase in agricultural yield is not significant enough to justify the greater expenditure on materials and the more complex installation required by deeper foundations to accommodate the increased wind loading experienced by taller structures.

4.2 Tracking Algorithm Impact on Yields

The study explored the impact of varying types of tracking algorithms on photovoltaic and agricultural yields, as developed in Annex B. Conducted in Spain, the specific case involved tomatoes under a 6m by 4-panel agrivoltaic setup on one hectare. These algorithms control the solar panels' light generation capabilities and the environmental conditions, impacting the dual yield of the agrivoltaic systems.

- **PV Prioritised Tracking System:** The first algorithm focuses predominantly on maximising solar yield, ceasing to track the sun only under conditions of extremely high wind for structural safety, and during high precipitation to avoid damage. This approach generated 1.13GWh per year and achieved a relative agricultural yield of 71% shown in Figure 5.
- **Agrivoltaic Tracking Algorithm:** The second algorithm makes further accommodations for environmental conditions; during periods of low precipitation, the panels are positioned vertically to maximise even water distribution to the crops below. This adjustment results in a slight decrease in electrical power generation but facilitates an additional 1% increase in crop growth due to extra light exposure during these rainy periods.
- **Crop-prioritised Algorithm:** The final algorithm prioritises crop growth, particularly during the key growth stages for tomatoes in June. The panels adjust their angles to maximise sunlight exposure to the crops, leading to an increase in plant growth of 7% while reducing solar output by 9%.

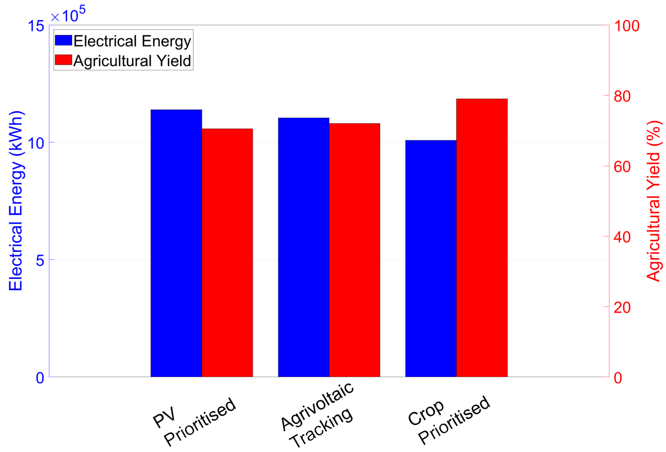

Figure 5: The impact of various tracking algorithms developed in Annex B on electrical and agricultural yield for an agrivoltaic installation in Spain growing tomatoes

4.2.1 Tracking Algorithm Discussion

The study validates the expected trend that reductions in solar tracking lead to increased sunlight exposure for crops and consequently, enhanced growth. This correlation is evident even with minor variations between PV-prioritised and agrivoltaic tracking algorithms. However, the model currently does not account for the added benefits of a more homogeneous distribution of light rain over the plants within the agrivoltaic algorithm. This is because the model primarily focuses on the total water balance of input against output. This represents an opportunity for future work to refine the tool by incorporating models that can assess the spatial distribution of water on crop yields more accurately.

Furthermore, the model effectively captures the benefits of crop-specific periods where anti-tracking can provide accelerated growth during crucial growth phases. This feature allows for the agrivoltaic system design to be adaptable to specific site requirements based on crop needs. Conversely, it supports purely solar tracking during periods when crops have sustained severe loss or damage, thereby helping protect the farmer's revenue by maximising electrical yield when agricultural yield is compromised.

This demonstrates the tool's versatility in dynamically balancing crop and electrical yields post-installation, allowing for tailored control over desired outputs. The agrivoltaic tracking algorithm is the preferred option for the application of this design due to the consistency of its yields, however, periods of anti-tracking during important crop growth periods should be assessed on a case basis. This flexibility is crucial for optimising agrivoltaic systems, ensuring sustainable and economically viable operations that maximise both energy production and agricultural productivity.

4.3 Row Spacing and Number of Panels Variables

Throughout this study, shading of the agrivoltaic structure on the crops and microclimate beneath has consistently been identified as the main influence on the output yields as a result of design choices. Furthermore, within Section 3.1 ground coverage ratio has been identified as the key influence on controlling the level of shade. Therefore the main influencing variables on GCR, the number of panels per module and the row spacing have been varied against each other to investigate how the two key variables impact final yields and can be selected for an optimised design. Figure 6 shows the results of this study for tomato growth in southern Spain. For layouts of minimum row spacing and a high number of panels which results in the densest arrays, the electrical yield is maximised, however, this minimises the agricultural yield, shown in Figure 6a. Conversely, sparse arrays with high row spacing result in maximum agricultural yield due to more irradiance reaching the crops, but minimum photovoltaic yield, as shown in Figure 6b. The significant influence of both variables on the outputs is clear, therefore the yields have been combined into one metric of land efficiency ratio (LER) shown in Figure 7, with the equation for LER found in Appendix E.1. LER is used to quantify improvements in land use [14], whereby an agrivoltaic system of 100 hectares with an LER of 1.6 would produce the same output as 160 hectares of separate agriculture and PV production land. It facilitates the selection of optimal agrivoltaic setup by overlaying constraints such as the two lines defining the region of variables where agricultural and electrical yield are at least 70% of the maximum possible yield, as was used in the case study application outlined in the group report aspect of this study, and visualised in Figure 7.

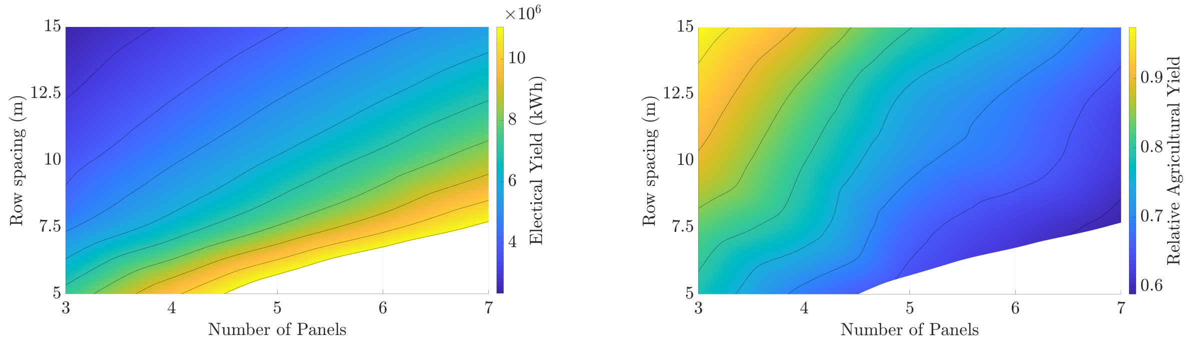

Figure 6: a) Yearly electrical energy yield, b) Relative agricultural output compared to pre-agrivoltaic installation as a function of the number of panels per module and inter-row spacing.

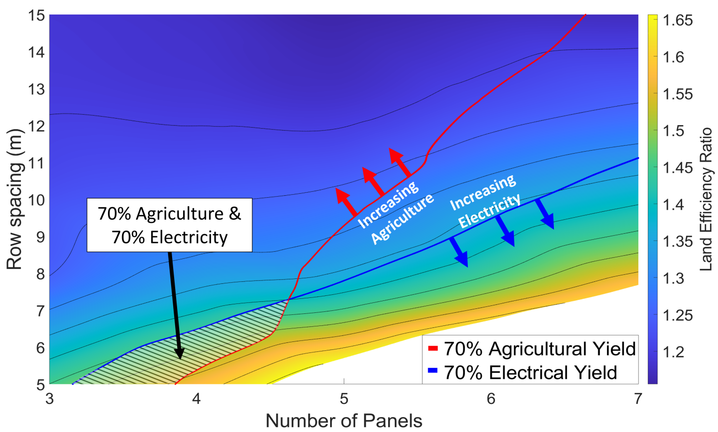

Figure 7: Land efficiency ratio as a function of the number of panels per module and inter-row spacing, with contours indicating 70% crop and electrical yield.

4.3.1 Discussion of Row Spacing and Number of Panels Study

The study identifies row spacing and the number of panels per module as key variables that significantly influence yields within agrivoltaic systems. Adjusting these parameters reveals a clear trade-off between maximising electrical and agricultural outputs, which is essential for optimising agrivoltaic system design. The introduction of the land efficiency ratio is crucial for selecting specific layouts, as it quantifies the effectiveness of land use and aids in balancing agricultural and photovoltaic outputs efficiently. By applying the LER, configurations that optimise land use can be identified, while adhering to site-specific constraints, such as the Italian government's guidelines requiring at least 60% of the site's potential photovoltaic output to be generated within agrivoltaics [15]. This approach provides a general framework for the strategic implementation of agrivoltaic systems, ensuring that both energy production and agricultural productivity are maximised under given environmental and regulatory conditions.

5 Conclusions

This project has successfully developed a comprehensive modelling tool specifically tailored for agrivoltaic system design, effectively merging the key elements of the separate modelling studies outlined in Annexes B and C to predict final electrical and agricultural yields. This bespoke model has undergone validation to ensure confidence in the predicted yields, with the fidelity of each modelling strand confirmed in Section 3. Furthermore, the integration of the modelling from separate annexes has been carefully assessed to ensure accuracy. The crop modelling's interaction with the microclimate modelling has been validated in Section 3.2, demonstrating the model's capability to accurately represent different water-stressed and irrigated conditions. Additionally, tracking mechanisms have been validated to confirm the model captures the appropriate impacts on yield for various algorithms. This comprehensive model now effectively supports the integration of its outputs with financial projections detailed in Annex E.

In this project, a range of variables were methodically adjusted to evaluate their impact on agrivoltaic system outputs and to aid in the selection of the optimal design. The adjustment of module height revealed that it is a less significant variable and should primarily be constrained by practical farming considerations, such as machinery clearance, rather than enhancing yield. Different tracking algorithms allowed for nuanced control over balancing agricultural and electrical yields, demonstrating effective management of energy maximisation versus crop growth optimisation. The most significant variables impacting outputs were identified as row spacing and the number of panels. Adjustments to these parameters dramatically affected both electrical and agricultural yields, enabling the exploration of a wide range of configurations. By plotting LER against configurations of row spacing and panel numbers, the model offered a clear framework to select the ideal setup that optimises land use while meeting both agricultural and electrical productivity requirements of the project. Overall, the development and application of this modelling tool justify its use in agrivoltaic planning and deployment. The model's flexibility and accuracy in optimising yields under various conditions make it invaluable for advancing agrivoltaic technologies, ensuring optimal agricultural productivity and energy generation in a sustainable and economically viable way.

Most of the modelling in this study focused on tomato growth in Spain, a region identified within the group report [16] as ideal for agrivoltaics both environmentally and economically. However, this means the analysis in this study does not fully exploit the modelling tool's versatility, such as accommodating 14 different annual crops and allowing for extensive customisation of location and agrivoltaic array variables. A significant challenge has been accessing detailed crop parameters and local climate data required for precise modelling. Therefore, while this study provides valuable insights, expanding the application of the model across a diverse range of environments remains a crucial aspect of future work and to prove the generality of the trends detailed. This expansion is vital to fully utilise the tool's capabilities and address the needs of a broader array of agrivoltaic applications worldwide, further ensuring the model's relevance and applicability in diverse agricultural and climatic conditions.

5.1 Recommendations and Further Work

Model versatility Testing: The future work identified in this study underscores the necessity to apply the modelling tool to a broader range of climates to fully test its capabilities. Achieving this will require extensive work to access detailed input parameters for a wide variety of environments. The first step towards this expanded application is set to commence imminently through participation in the AgriVoltaics World Conference 2024 Student Design Competition [17]. This opportunity will allow for testing the model's application in a new environment, specifically aimed at optimising fruit production and the food-water-energy nexus for a 10-hectare site in Colorado. Data retrieval for the site is already underway, with discussions opened with local farmers to obtain high-quality farming data. This initiative will provide the first opportunity to apply the model and its associated agrivoltaic framework to optimise the physical design for a specific site and demonstrate the effectiveness of the design in a practical setting.

User Interface and Financial Model Integration: A key area for future development involves integrating the agricultural modelling from this study with the financial modelling tools detailed in Annex E. The financial modelling tools have established a dynamic user interface that enables interactive access to cost predictions for various agrivoltaic site layouts. By merging this financial modelling with the current agrivoltaic system model, stakeholders can simulate and visualise the financial impacts of different agrivoltaic configurations in real time. The unified platform will support extensive scenario analysis, combining agricultural, electrical, and financial projections, which is essential for holistic and strategic agrivoltaic planning. This integration is a critical step towards developing a fully functional tool that addresses the multifaceted aspects of agrivoltaic systems.

References

[1] F. Panton, "Agrivoltaics - a yield prediction model for design optimisation," MEng Research and Development Dissertation, Faculty of Engineering, 2024.

[2] P. Loutzenhiser, H. Manz, C. Felsmann, P. Strachan, T. Frank, and G. Maxwell, "Empirical validation of models to compute solar irradiance on inclined surfaces for building energy simulation," Solar Energy, vol. 81, no. 2, pp. 254–267, 2007. [Online]. Available: https://www.sciencedirect.com/science/article/pii/S0038092X06000879

[3] C. Zhao, B. Liu, L. Xiao, G. Hoogenboom, K. J. Boote, B. T. Kassie, W. Pavan, V. Shelia, K. S. Kim, I. M. Hernandez-Ochoa, D. Wallach, C. H. Porter, C. O. Stockle, Y. Zhu, and S. Asseng, "A simple crop model," European Journal of Agronomy, vol. 104, pp. 97–106, 2019. [Online]. Available: https://www.sciencedirect.com/science/article/pii/S1161030118304234

[4] M. Tsubo and S. Walker, "Relationships between photosynthetically active radiation and clearness index at bloemfontein, south africa," Theoretical and Applied Climatology, vol. 80, pp. 17–25, 02 2005.

[5] R. Lindsey, "Climate change: Atmospheric carbon dioxide," Apr 2024. [Online]. Available: https://www.climate.gov/news-features/understanding-climate/climate-change-atmospheric-carbon-dioxide

[6] A. Weselek, A. Bauerle, J. Hartung, S. Zikeli, I. Lewandowski, and P. Högy, "Agrivoltaic system impacts on microclimate and yield of different crops within an organic crop rotation in a temperate climate," Agronomy for Sustainable Development, vol. 41, 10 2021.

[7] FAO, "Tomato," 2024. [Online]. Available: https://www.fao.org/land-water/databases-and-software/crop-information/tomato/en/

[8] AHDB, "Wheat growth guide," 2021. [Online]. Available: https://ahdb.org.uk/knowledge-library/wheat-growth-guide

[9] T. Huld, R. Müller, and A. Gambardella, "A new solar radiation database for estimating pv performance in europe and africa," Solar Energy, vol. 86, no. 6, pp. 1803–1815, 2012. [Online]. Available: https://www.sciencedirect.com/science/article/pii/S0038092X12001119

[10] "One building climate bristol weather file, https://climate.onebuilding.org/default.html, november 2022." [Online]. Available: https://climate.onebuilding.org/default.html

[11] Food and Agriculture Organization of the United Nations, "Tomato yields – FAO," with major processing by Our World in Data, 2023, production: Crops and livestock products [original data]. [Online]. Available: https://ourworldindata.org/grapher/tomato-yields

[12] Food and Agriculture Organization of the United Nations and Others, "Wheat yields," with major processing by Our World in Data, 2023, includes data from "Production: Crops and livestock products" by FAO; "Long-term crop yields in UK" by Broadberry et al. (2015); Brassley (2000); "Understanding Green Revolutions" by Bayliss-Smith & Wanmali (1984). [Online]. Available: https://ourworldindata.org/grapher/wheat-yields

[13] E. Vandest, "Agrisolar best practices guidelines version 2.0," Jun 2023. [Online]. Available: https://www.solarpowereurope.org/insights/thematic-reports/agrisolar-best-practice-guidelines

[14] C. Dupraz, H. Marrou, G. Talbot, L. Dufour, A. Nogier, and Y. Ferard, "Combining solar photovoltaic panels and food crops for optimising land use: Towards new agrivoltaic schemes," Renewable Energy, vol. 36, no. 10, pp. 2725–2732, 2011, renewable Energy: Generation Application. [Online]. Available: https://www.sciencedirect.com/science/article/pii/S0960148111001194

[15] M. dell'Ambiente e della Sicurezza Energetica, "Guidelines in the field of agri-voltaic systems," 2022. [Online]. Available: https://www-mase-gov-it.translate.goog/notizie/impianti-agri-voltaici-pubblicate-le-linee-guida?_x_tr_sl=it&_x_tr_tl=en&_x_tr_hl=en&_x_tr_pto=sc

[16] E. Balaban, E. Carey, J. Cooper, F. Panton, and A. Patel, "Agrivoltaics: Enabling a new market for solar pv projects," Project thesis, Faculty of Engineering, MEng in Engineering Design, Submitted in support of the degree of Master of Engineering, 4 2024, capstone Project, Project Advisor: Mervyn White, Department of Engineering, Partner Company: Everoze.

[17] AWC, "Agrivoltaics student design award," 2024. [Online]. Available: https://www.agrivoltaics-conference.org/program/agrivoltaics-student-design-award

[18] J.-B. Ornon, "Phenological stages: The key to understand and reduce the impact of climate change?" Apr 2023. [Online]. Available: https://climate.axa/phenological-stages-the-key-to-understand-and-reduce-the-impact-of-climate-change/#:~:text=What%20is%20a%20%E2%80%9Cphenological%20stage,back%2Dto%2Dback%20stages.

[19] P. Woli, J. W. Jones, K. T. Ingram, and C. W. Fraisse, "Agricultural reference index for drought (arid)," Agronomy Journal, vol. 104, no. 2, pp. 287–300, 2012. [Online]. Available: https://acsess.onlinelibrary.wiley.com/doi/abs/10.2134/agronj2011.0286

[20] W. Yao, Z. Li, Q. Zhao, Y. Lu, and R. Lu, "A new anisotropic diffuse radiation model," Energy Conversion and Management, vol. 95, pp. 304–313, 2015. [Online]. Available: https://www.sciencedirect.com/science/article/pii/S0196890415000205

Appendices

A Model Development

A.1 System Architecture

A.1.1 Modelling Inputs

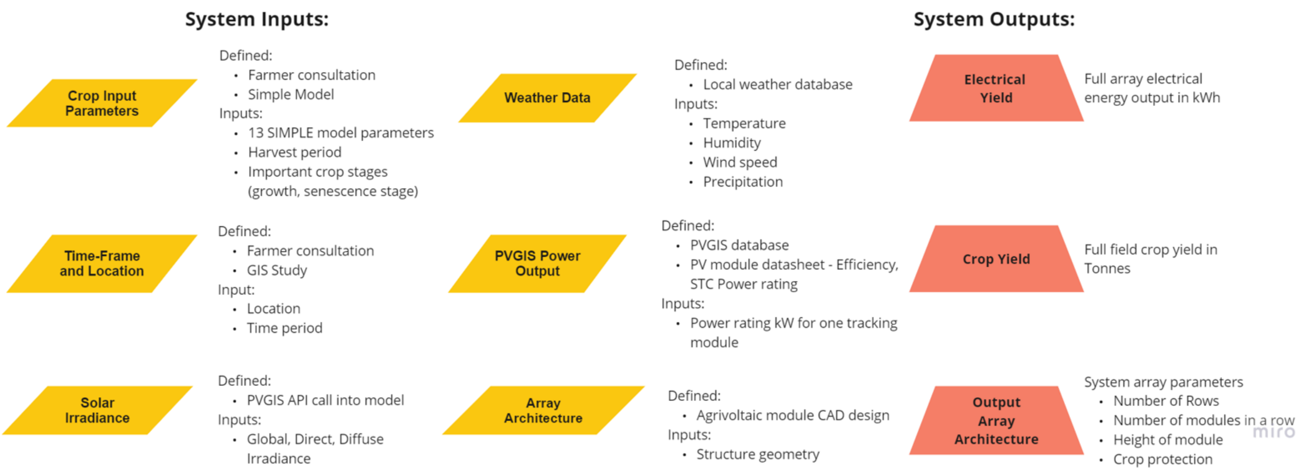

Figure 8: Complete list of input parameters and their source used to define a new case study investigation

A.1.2 Modelling Flow Chart

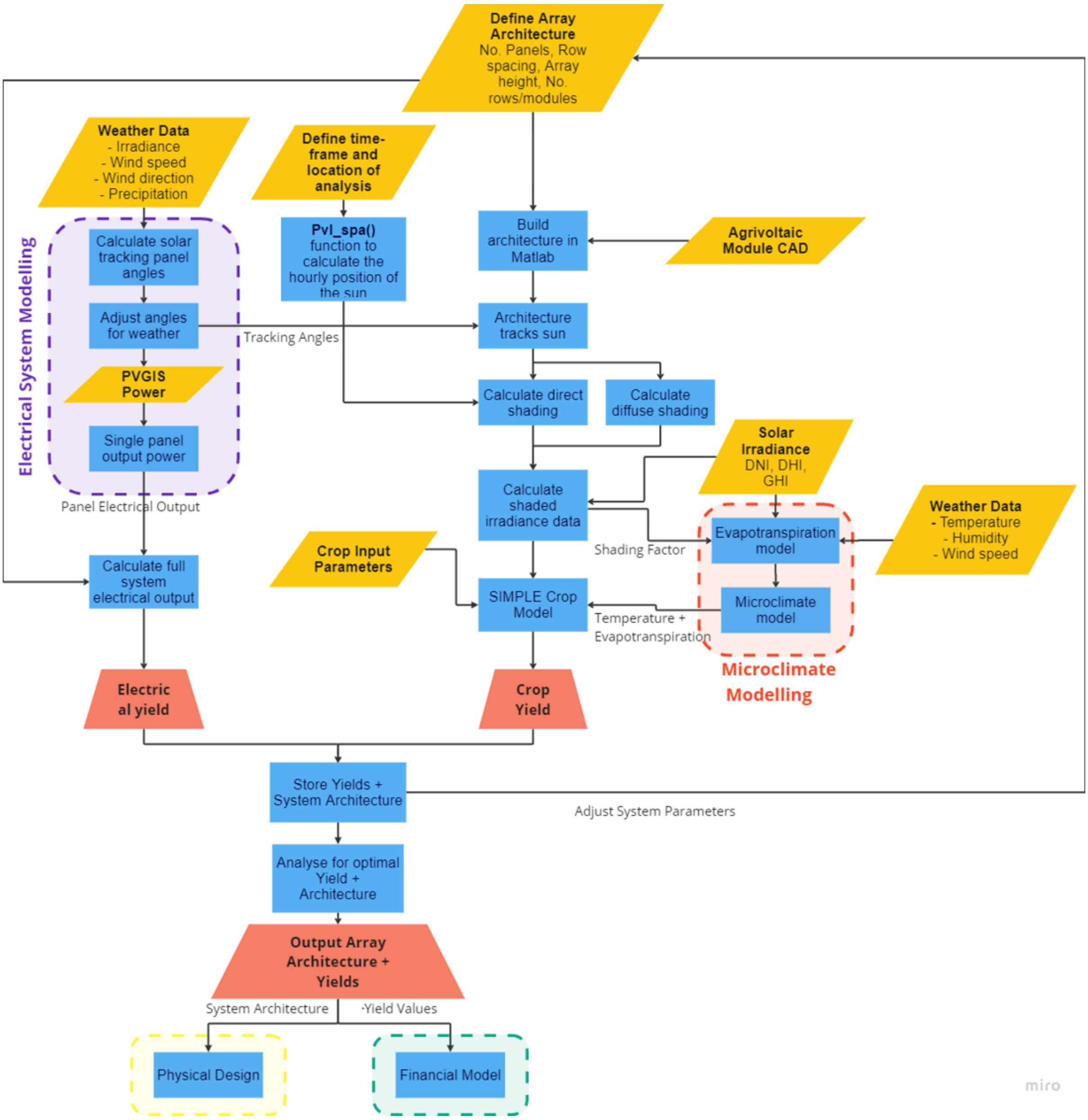

Figure 9: Algorithm flow diagram, showing the integration of the different modelling investigations into one larger tool and the information that flows between each model.

B Shading Modelling

B.1 Direct Irradiance Shadow Position Calculation

This appendix details the direct shading calculations for agrivoltaic modules, essential for determining the shadow projections on the ground. The projection of each vertex $\mathbf{P}_0$ of the agrivoltaic module onto the ground plane, $\mathbf{P}_s$, is calculated using the intersection of a line with a plane as follows:

$$\mathbf{p}_s = \mathbf{p}_0 - \frac{\mathbf{a} \cdot (\mathbf{p}_0 - \mathbf{v}_1)}{\mathbf{a} \cdot \mathbf{s}}$$

Where:

- **a** is the perpendicular unit vector to the ground plane, calculated by:

$$\mathbf{a} = (\mathbf{v}_3 - \mathbf{v}_1) \times (\mathbf{v}_2 - \mathbf{v}_1)$$

The geometrical components for this calculation are illustrated in Figure 10. Figure 10a visualizes the method for determining the projected shadow coordinate of a module vertex, and Figure 10b shows the overall shading scenario projected onto the ground.

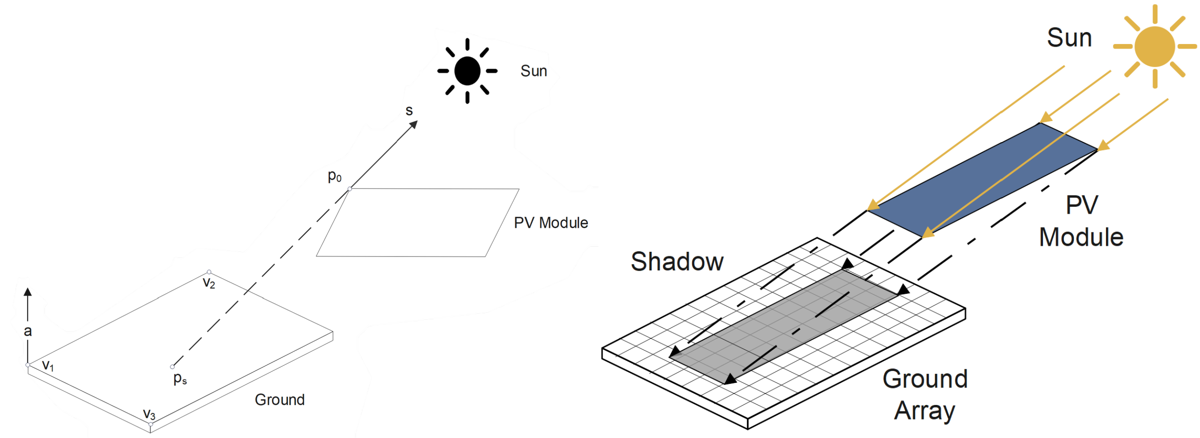

(a) The geometrical situation for calculating the projected shading coordinate of a panel vertex

(b) Visualisation of the shade projected onto a ground array

Figure 10: Visualisations of the shade calculation situation adapted from [1]

Once the shadow vertices are calculated, the next step involves determining which ground points are shaded. The shadow vertices are used to create a polygon of the shaded area. Each point on the ground is then tested to determine if it lies within this polygon using the `inpolygon` function in MATLAB. This process is repeated for each solar position within the designated time period, mapping the dynamically changing shaded areas. This approach offers a comprehensive evaluation of how agrivoltaic modules affect solar irradiance, crucial for understanding their environmental impact.

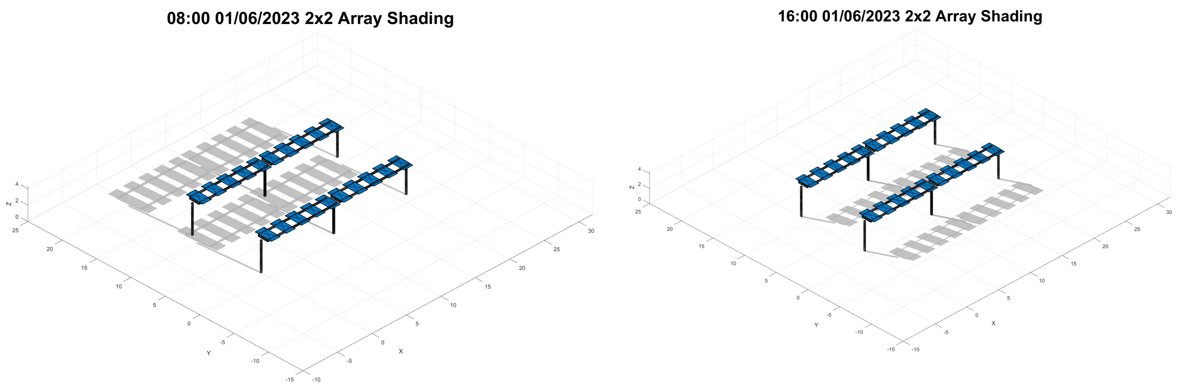

Figure 11: The difference in shadow position between 8am (left) and 4pm (right) for the first of June, with north positive in the x-axis and east negative in the y-axis.

B.2 Diffuse Irradiance Shading Factor Calculation

Diffuse light, which scatters from all directions in the sky, is influenced by the structural design of agrivoltaic modules. To estimate the reduction in diffuse irradiance, the ratio of the area covered by the agrivoltaic modules to the total boundary area of the array is calculated and visualised in Figure 13. This boundary includes both the panel plane area and the side areas of the array, providing a comprehensive measure of how much sky is obscured by the installation.

This ratio serves as an approximation of the reduction factor for diffuse irradiance, developed fro this model. By applying this reduction factor to the ambient diffuse irradiance at a given time, the exact amount of diffuse irradiance reaching the ground beneath the agrivoltaic structure can be accurately calculated. This method ensures that the impact of the agrivoltaic structure on light availability, crucial for crop growth beneath the modules, is precisely quantified. For a visual representation of how the agrivoltaic structure affects the diffuse light, refer to Figure 12.

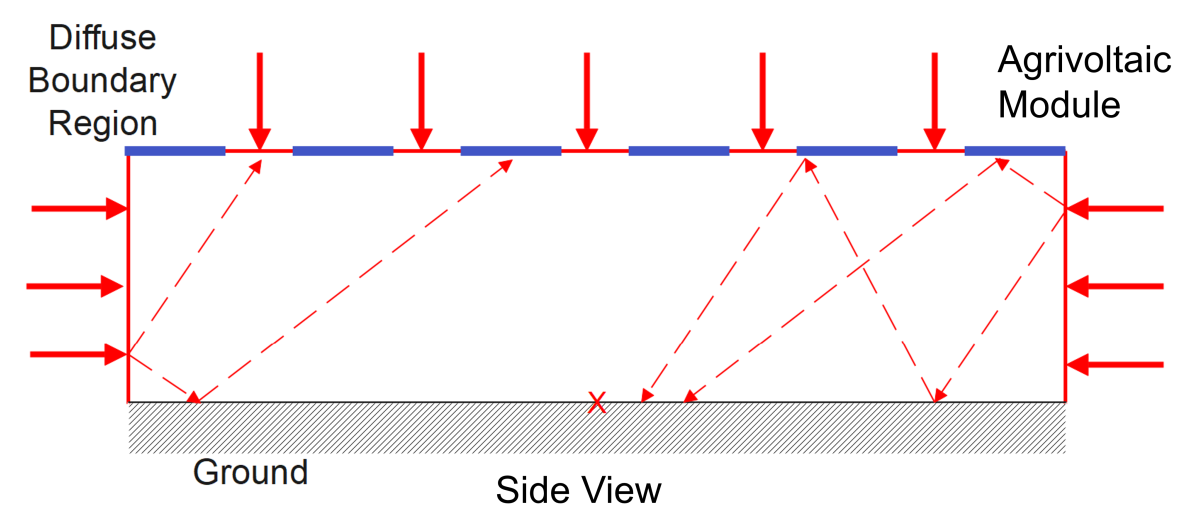

Figure 12: Side view of the diffuse irradiance boundary for an analysis point in the centre. Demonstrating the isotropic and random nature of diffuse irradiance

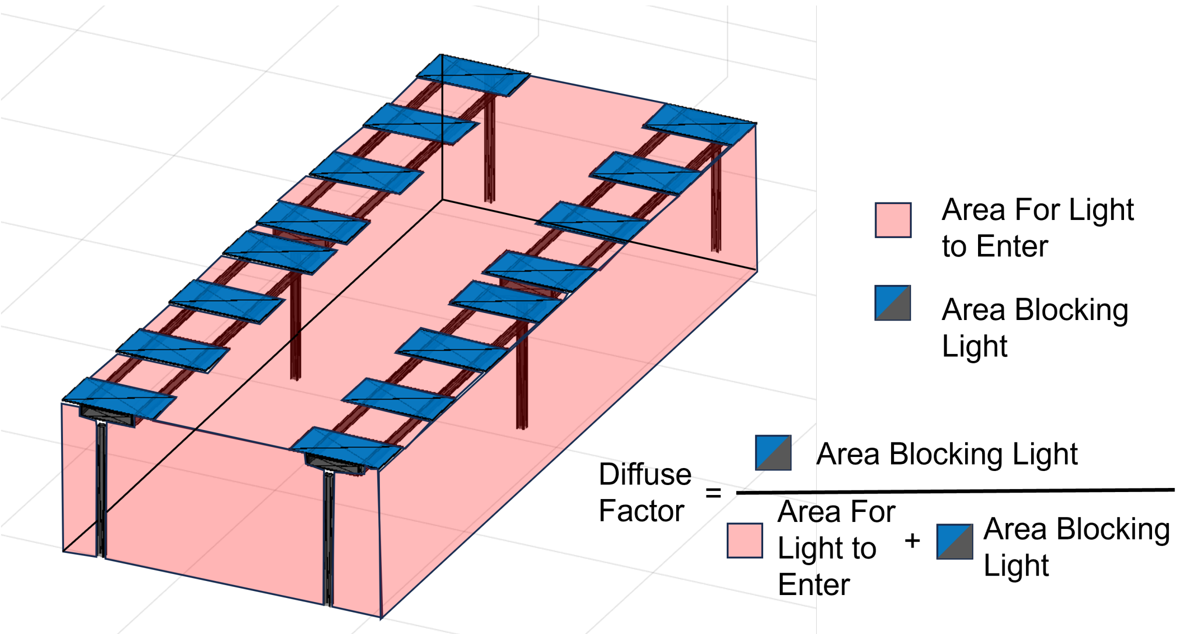

Figure 13: Visualisation on the Matlab generated agrivoltaic module, of the area of diffuse light blocked by a 2x2 module agrivoltaic structure (blue/black) and the total boundary area (red + blue/black), used to calculate the proportion of diffuse light blocked by the array.

C Crop Model Development

C.1 Summary of Key Equations and Variables

This Appendix provides a concise overview of the key equations and variables used in the agrivoltaic crop growth model established in Matlab. It includes mathematical formulas for biomass accumulation, phenological development, temperature impacts, heat stress, and the influence of CO_2 levels on crop yield. Each section briefly describes the equations involved, lists the relevant variables, and summarises their role in the model.

C.2 Crop Growth

Equations:

$$Biomass_{\text{rate}} = \text{Radiation} \times f_{\text{Solar}} \times \text{RUE} \times f(\text{CO}_2) \times f(\text{Temp}) \times \min(f(\text{Heat}), f(\text{Water})) \quad (1)$$

$$Biomass_{\text{cum},i+1} = Biomass_{\text{cum},i} + Biomass_{\text{rate}} \quad (2)$$

$$Yield = Biomass_{\text{cum, harvest}} \times \text{HI} \quad (3)$$

Variables:

- Radiation (Calculated): Daily received radiation calculated from the shading modelling and converted into photosynthetically active radiation by multiplying by 0.48 [4].
- f_{Solar} (Crop Specific): Fraction of solar radiation intercepted by the crop.
- RUE (Crop Specific): Radiation-use efficiency.
- $f(\text{CO}_2)$ (Calculated Variable): Function accounting for the effects of CO_2 concentration on crop growth.
- $f(\text{Temp})$ (Calculated Variable): Function accounting for the effect of temperature on crop growth.
- $f(\text{Heat})$ (Calculated Variable): Function representing the impact of heat stress on crop growth.
- $f(\text{Water})$ (Calculated Variable): Function representing the impact of water availability on crop growth.
- $Biomass_{\text{rate}}$ (Calculated Variable): Daily biomass growth rate.
- $Biomass_{\text{cum}}$ (Calculated Variable): Cumulative biomass.
- HI (Crop Specific): Harvest index, representing the ratio of harvestable to total biomass.

Summary: Crop yield is modelled as the product of cumulative biomass and harvest index, factoring in daily radiation, interception efficiency, and environmental stresses.

C.3 Phenological Development

Equations:

$$\Delta TT = \begin{cases} T - T_{\text{base}}, & T > T_{\text{base}} \\ 0, & T \leq T_{\text{base}} \end{cases} \quad (4)$$

$$TT_{i+1} = TT_i + \Delta TT \quad (5)$$

Variables:

- T (Model Output): Daily mean temperature, from the microclimate modelling in Annex C
- T_{base} (Crop Specific): Base temperature for phenological development.
- ΔTT (Calculated Variable): Daily increase in thermal time.
- TT (Calculated Variable): Cumulative thermal time.

Summary: Phenological stages [18] are determined by the accumulation of thermal time, which is the sum of daily temperatures above a species-specific base temperature, with temperature values sourced from the outputs of the microclimate modelling methods described in the algorithm.

C.4 Temperature Impact

Equation:

$$f(\text{Temp}) = \begin{cases} 0, & T < T_{\text{base}} \\ \frac{T - T_{\text{base}}}{T_{\text{opt}} - T_{\text{base}}}, & T_{\text{base}} \leq T < T_{\text{opt}} \\ 1, & T \geq T_{\text{opt}} \end{cases} \tag{6}$$

Variables:

- T (Weather Data): Daily mean temperature from the microclimate modelling in Annex C
- T_{base} (Crop Specific): Base temperature for growth.
- T_{opt} (Crop Specific): Optimal temperature for biomass growth.

Summary: The $f(\text{Temp})$ function integrates the impact of daily mean temperature on biomass growth, with all temperature values supplied as outputs from the microclimate modelling methods detailed in the algorithm. This function reflects inhibited growth when temperatures are below the base threshold and indicates optimal growth when temperatures reach or exceed the optimal range.

C.5 Heat Stress Impact

Equation:

$$f(\text{Heat}) = \begin{cases} 1, & T_{\text{max}} \leq T_{\text{heat}} \\ 1 - \frac{T_{\text{max}} - T_{\text{heat}}}{T_{\text{extreme}} - T_{\text{heat}}}, & T_{\text{heat}} \leq T_{\text{max}} \leq T_{\text{extreme}} \\ 0, & T_{\text{max}} \geq T_{\text{extreme}} \end{cases} \tag{7}$$

Variables:

- T_{max} (Weather Data): Daily maximum temperature from the microclimate modelling in Annex C
- T_{heat} (Crop Specific): Heat stress threshold temperature.
- T_{extreme} (Crop Specific): Extreme temperature for complete cessation of growth.

Summary: The $f(\text{Heat})$ function quantifies the impact of heat stress on biomass growth, decreasing linearly between the heat stress threshold and extreme temperature.

C.6 Drought Stress Impact

Equations:

$$f(\text{Water}) = 1 - S_{\text{water}} \times \text{ARID} \tag{8}$$

$$\text{ARID} = 1 - \frac{\min(ET_0, 0.096 \times \text{PAW})}{ET_0} \tag{9}$$

$$\text{PAW} = \frac{W_i}{\varsigma} = \frac{W_{i-1} + P_i + I_i - T_i - D_i - R_i}{\varsigma} \tag{10}$$

Variables:

- S_{water} (Crop Specific): Sensitivity of Radiation Use Efficiency to the ARID index.
- ARID (Calculated Variable): ARID index after Woli et al. (2012) [19], ranging from 0 (no water shortage) to 1 (extreme water shortage and drought stress).
- ET_0 (Weather Data): Reference evapotranspiration calculated in Annex C.
- W_i (Calculated Variable): Available water content on the ith day.
- P_i (Weather Data): Precipitation on the ith day.
- I_i (Irrigation Data): Irrigation applied on the ith day.
- T_i (Calculated Variable): Transpiration on the ith day calculated in Annex C.
- D_i (Weather Data): Deep drainage on the ith day.

- R_i (Weather Data): Runoff on the ith day.
- ς (Plant data): Root zone depth
- PAW (Calculated Variable): Plant available water

Summary: The function f(Water) assesses the impact of water availability and drought stress on crop growth by integrating the ARID index developed by Woli et al. [19], which reflects the severity of drought conditions and its consequent effect on the crop's Radiation Use Efficiency (RUE). The Plant-Available Water (PAW) is dynamically calculated based on daily water balance within the root zone. The calculations for evapotranspiration and transpiration are performed using the microclimate modelling methods described in Annex C, ensuring a comprehensive and dynamic assessment of water stress impacts on the crops.

C.7 CO_2 Impact

Function:

$$f(\mathrm{CO_2}) = 1.0923 \tag{11}$$

Variables:

- Current CO_2 level (Weather Data): 419ppm [5].
- Increase in crop yield (Calculated Value): Approximately 13% per 100ppm increase.

Summary: Elevated CO_2 levels enhance crop yield by improving photosynthetic efficiency, with the model reflecting an empirical increase of approximately 13% per 100ppm.

D Modelling Assumptions

D.1 Shading Assumptions

Table 3: Assumptions and Limitations in Shading Modelling

No.	Assumption	Reasoning/Justification	Possible Impact
1	Diffuse Irradiance is Isotropic	Assumes uniform distribution of diffuse light in all directions, common in radiation models. Validated by isotropic sky models for quantifying solar energy[2]. Treating diffuse irradiance as isotropic simplifies modelling calculations	If diffuse irradiance is not isotropic [20], it could indicate its influence by solar position, potentially altering shading values slightly.
2	Flat Ground Assumption	Assumes the ground beneath agrivoltaic modules is flat. Facilitates simpler geometrical calculations but may not accurately represent all installation sites, particularly those on uneven terrain, which could affect the accuracy of shadow projections.	Uneven or slanted terrain may lead to inaccurate shadow projections.
3	Uniform Panel Height	Assumes all panels are installed at the same height. Standardises shading pattern but does not account for possible variations in panel installation due to structural design or terrain irregularities.	Variation in panel height may lead to uneven shading, affecting the accuracy of shading predictions.
4	Static Sun Position	The model has to increment the sun's position and irradiance based on available data of hourly solar position and irradiance, not accounting for the continuous movement of the sun.	The direct shading calculations will have small rounding errors continuously, due to the variations in shading between the hour impacting the accuracy of shading predictions.
5	Simplification of PV Array Geometry	To make the modelling feasible the complete agrivoltaic module geometry has been simplified for modelling purposes. The modelling geometry does not contain components such as the motors, electrical cabling, control boxes, etc.	Simplifying module geometry may oversimplify, and slightly underestimate shading predictions, overlooking real-world components that could affect shading patterns.
6	Homogeneity of Crop Canopy	Assumes a homogeneous crop canopy under the agrivoltaic system. Simplifies analysis but does not account for variations in plant height, health, and density that can affect shading impact on crop growth.	Variations in crop canopy could lead to uneven shading effects, influencing crop growth differently across the field.
7	Constant Diffuse Reduction Factor	Assumes the reduction factor for diffuse irradiance is constant for a fixed panel setup throughout the year. Does not consider effects such as the tracking angle affecting diffuse shading and seasonal variations in sun angle and atmospheric conditions that influence diffuse light properties.	Seasonal variations in sun angle and atmospheric conditions may affect diffuse light properties, impacting the accuracy of diffuse irradiance calculation.
8	Ignoring Edge Effects	The model may not fully account for edge effects, where the interaction between the edge of the agrivoltaic structure and the open environment could create different microclimatic conditions and allow more diffuse light through the sides of the array	Neglecting edge effects may overestimate shading effects and overlook microclimatic variations, affecting crop growth predictions.
9	Neglect of Environmental Variables	Additional environmental factors such as wind, precipitation, and cloud cover are not explicitly accounted for in shading calculations, which might affect the actual irradiance and microclimate conditions experienced by the crops.	Neglecting environmental variables may lead to an incomplete assessment of shading effects and microclimate conditions, impacting crop growth predictions. However, selecting thorough weather data sources in PVGIS should minimise the impacts of this.

D.2 Crop Modelling Assumptions

Table 4: Assumptions and Limitations in Crop Modelling

No.	Assumption/	Reasoning/Justification	Possible Impact
1	Constant CO2 Levels	Assumes that the plant CO2 concentration remains stable throughout the modelling period at atmospheric levels, simplifying the CO2 availability function, which can affect plant growth and photosynthesis rates.	There could be a reduction in CO2 levels under the agrivoltaic structure for more dense arrays due to less airflow which could slightly reduce plant growth.
2	Uniform Irrigation	Where irrigation has been applied to the modelling it assumes uniform irrigation practices across the crop field, simplifying the modelling process by neglecting variations in water availability and irrigation methods.	Variations in water availability and irrigation methods may lead to uneven crop growth and yield, affecting model accuracy.
3	Uniform Soil Composition	Assumes uniform soil composition and properties across the crop field. This simplifies the modelling process by neglecting variations in soil characteristics, such as nutrient levels and moisture retention.	Variations in soil characteristics can lead to differences in nutrient availability and water retention, impacting crop growth and yield predictions.
4	Homogeneous Crop Canopy	Assumes a homogeneous crop canopy across the field. This simplifies analysis but may not accurately represent real-world conditions where variations in plant height, health, and density exist, affecting light interception.	Variations in crop canopy density and height can lead to differences in light interception and crop growth, influencing model accuracy.
5	Vernalization Response	The model does not consider the effects of vernalization on crop phenology, which can be important for some crops and cultivars such as carrots.	Ignoring vernalization effects may lead to incorrect predictions of crop development stages and maturity timing, impacting harvest scheduling and yield estimation.
6	Photoperiod Effect on Phenology	The model does not consider the effects of photoperiod on crop phenology, which can be important for some crops and cultivars.	Ignoring photoperiod effects may lead to incorrect predictions of crop development stages and maturity timing, impacting harvest scheduling and yield estimation.
7	Lack of Crop Nutrient Dynamics	The model does not account for crop nutrient dynamics due to the significant complexity and local input data required.	Ignoring crop nutrient dynamics may be less important for high-value fruit and vegetable crops in industrial countries, which are supplied sufficient nutrients, but can be significant in some developing countries with limited nutrient inputs. This limitation may lead to an underestimation of yield or growth potential in nutrient-deficient soils.
8	Exclusion of Frost, Pest, and Disease Impacts	The model does not consider the impacts of frost, pests, and diseases on crop growth and yield, similar to many other crop models.	Neglecting frost, pest, and disease impacts can lead to underestimation of yield losses, especially in regions with high pest and disease prevalence, affecting model accuracy in such environments.

E Results

E.1 Combined Indicator: Land Efficiency Ratio

The land efficiency ratio (LER) serves as an indicator of land productivity when multiple production systems share the same land. Originally proposed by Dupraz et al. [14] for application in agrivoltaic scenarios, it combines the yields of both crop production and electrical output. Equation 12 defines the LER as:

$$LER_{sn} = \frac{Y_{crop.calc}}{Y_{crop.full}} + \frac{Y_{kWh.calc}}{Y_{kWh.full}}. \tag{12}$$

In this study, the LER is employed to compare the calculated crop yields ($Y_{crop.calc}$) to a yield obtained under full sun conditions ($Y_{crop.full}$). Similarly, the electrical yield ($Y_{kWh.calc}$) is compared to a reference yield ($Y_{kWh.full}$) representing optimal layout conditions for maximising electrical output. The reference yield is determined as the maximum electrical yield provided by the model before the coverage becomes too dense and causes inter-row shading.